High-order harmonic generation from H_2^+ irradiated by a co-rotating two-color circularly polarized laser field

Yue Qiao,[1,2] Dan Wu,[1,2] Ji-Gen Chen,[3] Jun Wang,[1,2,*] Fu-Ming Guo,[1,2,†] and Yu-Jun Yang[1,2,‡]

[1]*Institute of Atomic and Molecular Physics, Jilin University, Changchun 130012, China*

[2]*Jilin Provincial Key Laboratory of Applied Atomic and Molecular Spectroscopy (Jilin University), Changchun 130012, China*

[3]*Department of Materials Engineering, Taizhou University, Taizhou 318000, China*

(Received 31 May 2019; revised manuscript received 9 December 2019; published 30 December 2019)

The high-order harmonic generation process of H_2^+ in a co-rotating two-color circularly polarized laser pulse was investigated by numerically solving the time-dependent Schrödinger equation. Compared with the target of the atom, the harmonic intensity of H_2^+ is remarkably enhanced. Moreover, the harmonic intensity of H_2^+ approaches its maximum when the electric field amplitude ratio of the fundamental frequency and the second one is approximately 1:2.3. By analyzing the evolution of the time-dependent wave packets, the enhancement of harmonic intensity may be attributed to an increase in the probability of the ionized electron recolliding with the parent ion. In addition, the dependence of harmonic intensity on the internuclear distance and the alignment angle of H_2^+ is explored. We found that the ellipticity of the particular harmonic order changes with the molecular alignment angle, which provides a chance to generate an extreme ultraviolet coherent light pulse with controllable polarization.

DOI: 10.1103/PhysRevA.100.063428

I. INTRODUCTION

High-order harmonic generation (HHG) from atoms and molecules in an intense laser pulse is a coherent light source with the spectra from extreme ultraviolet (XUV) to soft x ray [1–6]. Owing to its wide spectrum, HHG is an important way to produce optical pulses with an attosecond duration (10^{-18} s) [1,7–11]. As HHG is generated by the collision of the ionized electron with its parent ion in the laser electric field, the harmonic spectrum carries the structural properties of the atomic and molecular ion. Therefore, HHG can be used as a detector for a static and dynamic molecular structure [12–17].

According to the three-step model of the harmonic generation process, the ionized electron recombines with the parent ion and releases the gained energy by radiating a harmonic photon. On the basis of the model, when an atom is driven by a linearly polarized laser field, the ionized electron moves in a one-dimensional space, and harmonic polarization is linear as a result of the recollision of the ionized electron with the parent ion along the polarized direction of the driven laser pulse. If the driving pulse is a circularly polarized laser field, the ionized electron moves in a two-dimensional plane, and the direction of the electron's velocity changes with time, which leads to an ionized electron with fewer chances to recollide with its parent ion; therefore, the harmonic intensity is very low [18,19]. However, when an atom is irradiated by a counter-rotating two-color circularly polarized laser pulse, the ionized electron can return back to the parent ion from different angles, and the strong circularly polarized harmonic radiation could be observed in experiment [20]. The circularly polarized harmonics were applied to the magnetic circular dichroism measurement of Co [21]. Owing to the potential application of circularly polarized harmonics in the measurement of magnetic materials and chiral molecules, the effects of laser parameters on the harmonic intensity and the polarization were further studied in recent years [22–26].

Compared with studies on HHG from the counter-rotating two-color circularly polarized laser, there are fewer studies on HHG of an atom or a molecule in the co-rotating two-color circularly polarized (CRTCCP) laser pulse. In 1995, Becker *et al.* initially examined HHG from an atom irradiated by the CRTCCP laser [27], and they illustrated that HHG is caused by high-order difference-frequency mixing processes, and the harmonic signal decreases rapidly with the increase of the harmonic order. In 2000, on the basis of a strong-field approximation scheme, Milosevic *et al.* reported that the harmonic intensity from the hydrogen atom in the CRTCCP field is weaker than that of the counter-rotating two-color circularly polarized laser field [28]. Sharma *et al.* studied the generation of even and odd harmonics by the propagation of co-rotating and counter-rotating two-color circularly polarized laser beams through homogeneous, underdense plasma and found that the normalized amplitudes of the harmonics are approximately the same as those obtained by the two-color linearly polarized laser beams [29]. Recently, a study on the double ionization of the atom and the molecule provided a possibility to produce a high-intensity harmonic by using a CRTCCP field. Hang *et al.* found the nonsequential double-ionization yield of the atom can be changed by adjusting

*wangjun86@jlu.edu.cn
†guofm@jlu.edu.cn
‡yangyj@jlu.edu.cn

the amplitude ratio of the CRTCCP field [30]. Busuladžić *et al.* theoretically investigated the photoelectron emission spectra of the aligned N_2 and confirmed the contribution of rescattered electrons in the CRTCCP laser field [31]. Whether the electrons rescattered in the CRTCCP field will produce efficient HHG is the content of this paper.

In this work, we have focused on HHG from the molecule in the CRTCCP laser pulse and the features of the harmonic spectra. By adopting the numerical solution of the time-dependent Schrödinger equation (TDSE), the dynamic process of the molecular HHG in the CRTCCP laser pulse was performed. We found that the harmonic intensity is enhanced for a specific amplitude ratio of the CRTCCP laser field, which can be explained by utilizing the wave-packet evolution and the classical trajectory analysis. In Sec. II, the numerical method and theoretical scheme for calculating the harmonic spectrum are discussed. In Sec. III, we show the results and provide some discussions. This article is summarized in Sec. IV, and atomic units are used throughout this paper unless specified otherwise.

II. THEORETICAL MODEL AND NUMERICAL METHOD

Under electric dipole approximation and length gauge, the TDSE of $H_2{}^+$ driven by the CRTCCP laser pulse is

$$i\frac{\partial}{\partial t}\psi(x,y,t)=\hat{H}(x,y,t)\psi(x,y,t). \tag{1}$$

The Hamiltonian in Eq. (1) is

$$\hat{H}(x,y,t)=\frac{p_x^2+p_y^2}{2}+V(x,y)+xE_x(t)+yE_y(t). \tag{2}$$

The soft-core Coulomb potential can be expressed as

$$V(x,y)=-\frac{1}{\sqrt{(x-\frac{R}{2}\cos\theta)^2+(y-\frac{R}{2}\sin\theta)^2+a(R)}} -\frac{1}{\sqrt{(x+\frac{R}{2}\cos\theta)^2+(y+\frac{R}{2}\sin\theta)^2+a(R)}}, \tag{3}$$

where R is the internuclear distance, and $a(R)$ is the soft-core parameter. The soft-core parameter is called $a(R)$ as it is necessary to adjust the soft-core parameter to ensure that the ionization energy at a different R of the molecule is consistent with the ionization energy of the real molecule. For example, when $R=3.2$, $a(R)=0.68$; then the ionization energy is about 24 eV [32]. θ is the angle between the molecular axis and the x axis. The electric field vector of the CRTCCP pulse $E(t)=E_x(t)\hat{e}_x+E_y(t)\hat{e}_y$ was chosen to rotate in the x-y plane. $E_x(t)$ and $E_y(t)$ are the x and y components of the laser field, respectively. The detailed form of the laser electric field used in this work is as follows:

$$E_x(t)=E_0f(t)\left[\left(\frac{1}{1+\varepsilon}\cos(\omega t)\right)+\left(\frac{\varepsilon}{1+\varepsilon}\cos(2\omega t)\right)\right],$$
$$E_y(t)=E_0f(t)\left[\left(\frac{1}{1+\varepsilon}\sin(\omega t)\right)+\left(\frac{\varepsilon}{1+\varepsilon}\sin(2\omega t)\right)\right]. \tag{4}$$

The $f(t)$ is the laser pulse envelope with a duration of eight optical cycles. The shape of the envelope is trapezoidal, with a one-cycle linear turn-on and a one-cycle linear turn-off. E_0 and ω are the peak amplitude and the frequency of the laser pulse, respectively. Furthermore, ε is a parameter used to adjust the amplitude ratio between the fundamental field and the second harmonic laser. The electric field amplitude ratio of the fundamental frequency and the second one is $1{:}\varepsilon$.

A time-dependent wave function was obtained through the numerical solution of Eq. (1) with a splitting-operator fast-Fourier-transform scheme [33–37]. To avoid unphysical reflection of the wave packet from the boundary, the wave function was multiplied by a $\cos^{1/8}$ mask function at each time step. By using the time-dependent wave function, the dipole accelerations in the x and y directions are written as

$$a_x(t)=\frac{d^2}{dt^2}\langle\psi(x,y,t)|x|\psi(x,y,t)\rangle =\left\langle\psi(x,y,t)\left|-\frac{\partial V(x,y)}{\partial x}-E_x(t)\right|\psi(x,y,t)\right\rangle,$$
$$a_y(t)=\frac{d^2}{dt^2}\langle\psi(x,y,t)|y|\psi(x,y,t)\rangle =\left\langle\psi(x,y,t)\left|-\frac{\partial V(x,y)}{\partial y}-E_y(t)\right|\psi(x,y,t)\right\rangle. \tag{5}$$

The corresponding harmonic spectra are calculated by

$$P_{a_x}(\omega)=\left|\frac{1}{\omega^2(t_n-t_0)}\int_{t_0}^{t_n}a_x(t)e^{-i\omega t}dt\right|^2,$$
$$P_{a_y}(\omega)=\left|\frac{1}{\omega^2(t_n-t_0)}\int_{t_0}^{t_n}a_y(t)e^{-i\omega t}dt\right|^2. \tag{6}$$

In order to explain the observed harmonics, the classical Monte Carlo model [38] was adopted to analyze the recollision probability of $H_2{}^+$ in the CRTCCP field. In this model, the electronic movement in $H_2{}^+$ is followed by Newton's equation:

$$\ddot{x}=-\frac{\partial V(x,y)}{\partial x}-E_x(t),$$
$$\ddot{y}=-\frac{\partial V(x,y)}{\partial y}-E_y(t). \tag{7}$$

III. RESULTS AND DISCUSSION

A. The enhancement of harmonic intensity of $H_2{}^+$ in the co-rotating two-color circularly polarized laser field

In Fig. 1(a), we present the harmonic spectra of the atom (the dashed black line) and $H_2{}^+$ (the solid red line) irradiated by the CRTCCP laser pulse. The wavelength of the fundamental field is 800 nm, and the laser field peak amplitude E_0 is 0.092, corresponding to $I=3\times10^{14}\mathrm{W/cm^2}$. When the amplitude ratio of the two-color pulses is 1:1, the atomic harmonic intensity is extremely low [see Fig. 1(a)]. With the increase of the harmonic order, its intensity decreases rapidly. The harmonic intensity can be controlled by the amplitude ratio of the two pulses. We found that the harmonic intensity is the largest when $\varepsilon=2.3$. For the 15th harmonic, the harmonic intensity of $\varepsilon=2.3$ is about an order of magnitude higher than that of $\varepsilon=1$. This finding is similar to previous studies of double-ionization enhancement of atoms [30]. In the case of the harmonic spectrum from $H_2{}^+$ irradiated by the same pulse,

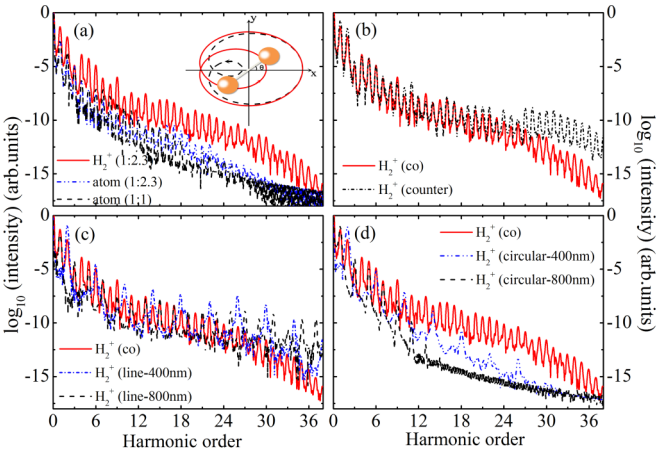

FIG. 1. Comparison of harmonics generated by H_2^+ and the atom under different forms of driving lasers. (a) Harmonic spectra of H_2^+ and the atom by the co-rotating two-color circularly polarized laser. The inset shows the electric fields of the CRTCCP laser when the amplitude ratios are 1:2.3 (solid red line) and 1:1 (dashed black line), and the counterclockwise rotation direction of the two fields is marked with red and black arrows, respectively. The angle between the molecular axis and the x axis is also depicted here. (b) The harmonic spectra of H_2^+ by the co-rotating (solid red line) and counter-rotating (dash-dotted black line) two-color circularly polarized lasers. (c) The harmonic spectra of H_2^+ by the co-rotating two-color circularly polarized field using an 800–400-nm laser pulse (solid red line) and linearly polarized 800-nm (dashed black line) and 400-nm (dash-dotted blue line) lasers. (d) The harmonic spectra of H_2^+ by the co-rotating two-color circularly polarized field using an 800–400-nm laser pulse (solid red line) and circularly polarized 800-nm (dashed black line) and 400-nm (dash-dotted blue line) lasers.

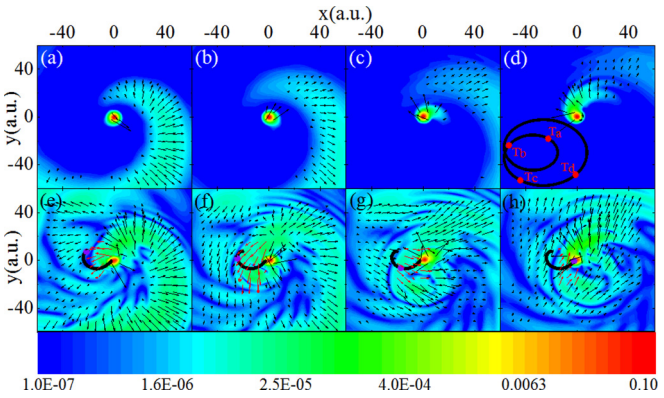

FIG. 2. The wave-packet motion of (a)–(d) the atom and (e)–(h) H_2^+ at different times T_a, T_b, T_c, and T_d in the co-rotating two-color circularly polarized laser. The arrow indicates that the electron probability flow and the solid black lines in (e)–(h) all represent the classic electronic trajectory of the T_a–T_d period, where the purple dot indicates the electronic position at the corresponding time, and the electric fields of the corresponding four moments are shown as the red dot in the solid black line of (d).

it is found that the harmonic intensity is high when the angle θ between the molecular axis and the x axis of the laser field is equal to 15°, and the internuclear distance is $R = 3.2$. The variation of harmonics with the internuclear distance and the alignment angle is further discussed in Sec. III C. The H_2^+ harmonic spectrum exhibits a clear plateau with even and odd ordered harmonics. Comparing with the harmonic from the atom, the harmonic intensity of H_2^+ is enhanced by about three orders of magnitude.

In addition, we gave the harmonic spectra generated by H_2^+ at $R = 3.2$, $\theta = 15°$, under different laser fields, as shown in Figs. 1(b)–1(d). In Fig. 1(b), we calculated the harmonic spectra of the co-rotating and counter-rotating two-color circularly polarized laser pulses with the same laser parameters and $\varepsilon = 2.3$. The previous results demonstrated that the harmonic intensity of atoms in the CRTCCP laser field was far lower than that of the counter-rotating two-color circularly polarized laser field. However, harmonic intensities of molecules in the co-rotating (solid red line) and counter-rotating (dash-dotted black line) two-color circularly polarized laser pulses are comparable. In general, the harmonic intensity of the CRTCCP laser field is slightly lower than that of the counter-rotating two-color circularly polarized laser field. However, at some particular orders, the harmonic intensity of the CRTCCP laser field could be higher than that of the counter-rotating two-color circularly polarized laser field. Figure 1(c) shows the harmonic spectrum comparison of H_2^+ under the CRTCCP field using an 800–400-nm laser pulse (solid red line) and linearly polarized 800-nm (dashed black line) and 400-nm (dash-dotted blue line) lasers. From the comparison of the harmonics of the CRTCCP field and the linear polarization field in Fig. 1(c), it can be seen that the harmonics of the CRTCCP field can reach the equivalent intensity of the linear polarization even though the intensity at some order exceeds that of the linear polarization. Moreover, odd and even harmonics appear in the case of the co-rotating two-color circularly polarized field. In addition, Fig. 1(d) shows the comparison of harmonic spectra in the CRTCCP field and the monochromatic circular polarization field. The harmonic intensities of the circular polarization at 400-nm (dash-dotted blue line) and 800-nm (dashed black line) laser pulses are very low. The harmonic in the CRTCCP (solid red line) field has several orders of higher magnitude intensity than the others.

According to the above discussions, the harmonics of H_2^+ driven by the CRTCCP laser field are different from the harmonics of atoms in the commonly known CRTCCP field. The harmonic intensity of H_2^+ driven by the CRTCCP laser field is not always low, and it can near the harmonic intensity of the counter-rotating two-color circularly polarized laser field and the monochromatic linear polarization field at a suitable double-circle amplitude ratio. In some orders, intensities are even stronger. In the following, we focused on the mechanism of harmonic generation in the co-rotating two-color circular polarization field in this paper.

B. Harmonic generation mechanism

In order to understand the high-intensity harmonics generated in the interaction between H_2^+ and the CRTCCP laser pulse, we present the time-dependent evolution of the H_2^+ wave packet, as shown in Figs. 2(e)–2(h). For comparison, the wave-packet evolution of the atom is also shown in

Figs. 2(a)–2(d). In Fig. 2, the time domain changes from $2.56T$ (where T is the optical cycle of the fundamental laser) to $2.94T$, with an interval of $0.12T$, and electric fields at four corresponding instants: T_a, T_b, T_c, and T_d, which are depicted in Fig. 2(d). One can see from Fig. 2 that ionized wave packets of the atom [Figs. 2(a)–2(d)] and the molecule [Figs. 2(e)–2(h)] rotate counterclockwise by the laser field, and the rotation direction is the same as that of the electric field vector. This is consistent with the behavior of classical charged particles driven by the same laser pulse. The electronic wave-packet distributions of the molecule [Figs. 2(e)–2(h)] and the atom [Figs. 2(a)–2(d)] appear significantly different. In the case of the atom, the ionized electron wave packet is produced near the nucleus, and then it gradually moves away from the nuclear region. Although the wave packet diffuses with gradual time, there remains no visible component of the wave packet, which can collide with the parent ion. Owing to the low recollision probability of the ionized electron colliding with the parent ion, the intensity of the HHG from the atom is extremely low. However, the ionized wave packet of the molecule has a more pronounced dispersion effect. There is a clear distribution of ionized electron wave packets in the nuclear region at a specific time, which means that there is a possibility of higher harmonic emissions under such conditions.

In order to understand this process more, we gave one of the classic trajectories returning to the nuclear region, which is a main contributor to the harmonic emission, as shown in Figs. 2(e)–2(h). The purple circle denotes the classical position of the ionization electron at the corresponding instant. At the same time, the spatial distribution of the electron probability stream obtained by the electron wave function is given as $\vec{j} = \frac{1}{2}[\psi^* \hat{p} \psi - \psi \hat{p} \psi^*]$, indicated by the arrow in Fig. 2. The direction of the arrow represents the direction of the movement of the ionized electrons, and the length of the arrow represents the magnitude of the flow rate. In the case of the atom, the electron probability flow rate and positions are generally away from the nuclear region. This indicates that the electrons are always moving away from the nuclear region, and it is difficult to generate high-order harmonics in collision. For the molecule, there is a component in which the electrons initially move away from the nuclear region and then return to the nuclear region, as shown by the area marked by the red arrow. It is clear that the direction of the electron probability flow rate changes to the left after ionization at time T_a in Fig. 2(e), which indicates that the electron moves to the left and away from the nuclear region. As time passes, the electrons at T_b, T_c, and T_d move to the lower left, lower right, and upper right, respectively, before returning to the nuclear region. During the T_a–T_d periods, the wave-packet motion behavior reflected by the probability flow is consistent with the electronic motion behavior of the classical trajectory.

To understand the enhancement of the molecular harmonic intensity, we systematically studied the effect of amplitude ratios of the CRTCCP laser field on the harmonics in the plateau region. Figure 3(a) exhibits the variation of the 25th to 30th harmonic intensity for different amplitude ratios. The laser field peak amplitude is 0.16, corresponding to $I = 8 \times 10^{14}$ W/cm^2. The internuclear distance of H_2^+ is $R = 2$, and the angle θ is 0°. Figure 3(a) demonstrates that the amplitude

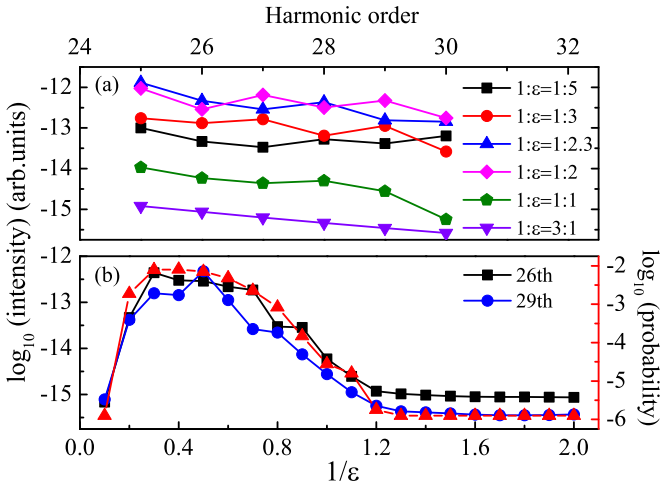

FIG. 3. (a) HHG of H_2^+ in the CRTCCP laser pulse with different amplitude ratios. (b) The 26th (black square) and 29th (blue circle) harmonic intensity, and the recollision probability (red triangle) as a function of the amplitude ratio.

ratio 1:ε influences the molecular harmonics in the plateau region. When the amplitude ratio is approximately 1:2.3, the harmonic intensity is generally higher, and when the amplitude ratio is 3:1, the harmonic intensity is generally lower. There are about three orders of magnitude in the harmonic intensity between both cases. Furthermore, considering the 26th and 29th harmonics as examples, we examined the harmonic intensity as a function of the amplitude ratio, as shown in Fig. 3(b). With an increasing amplitude ratio, the harmonic intensity initially increases, reaching a maximum at 0.3–0.5, and then it begins to gradually decrease. When the amplitude ratio is larger than 1.2, the harmonic intensity does not change substantially.

In order to clearly explain the variation in the harmonic intensity, we calculated the recollision probability of the ionized electron at different amplitude ratios using the classical Monte Carlo method, as shown by the red triangle in Fig. 3(b). In this classical calculation, the initial position and momentum of the electron distribute randomly in the molecular potential. The ionization probability is calculated from the electronic energy at the end of the driving laser pulse. Figure 3(b) shows that the variations in the recollision probability and the harmonic intensity with the amplitude ratio are almost identical.

To explore the harmonic generation's dynamic process of H_2^+ in the CRTCCP laser pulse, we calculated the electronic classical trajectories for different amplitude ratios. Figures 4(a)–4(d) show the instantaneous variations of the electric field vector with different amplitude ratios. Figures 4(e)–4(h) present the trajectories of the ionized electron of the corresponding laser fields in Figs. 4(a)–4(d), respectively. The line's color indicates the different ionization instances. Compared with the quantum results in Figs. 2(e)–2(h), more ionized electrons return to the parent ion region (near the coordinate origin) at an amplitude ratio of 1:2.3. For this laser field, the recollision electron is generated at the vicinity of the maximum value of the inner field, as shown by the green part in Fig. 4(b).

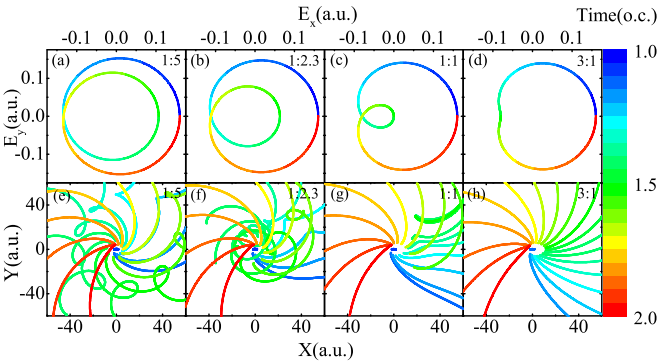

FIG. 4. (a)–(d) The instantaneous variations of the electric field vector with different amplitude ratios; (e)–(h) classical motion trajectories in different ionization instants at one optical cycle for different amplitude ratios.

C. Influence of the internuclear distance and the alignment angle on the harmonics of H_2^+

According to the above discussion, the harmonic intensity depends on the ionization and recollision probability of the ionized electron. The ionization and recollision probability are affected by the internuclear distance of the molecule. Therefore, the HHG spectrum can be altered. Figure 5(a) shows the harmonic spectra of H_2^+ with internuclear distances of $R = 2$ and $R = 3.2$ under the CRTCCP laser pulse with an amplitude ratio of 1:2.3. Figure 5(a) shows that the intensity of the overall harmonic emission spectrum from $R = 3.2$ is significantly stronger than that from the molecular ion with a small internuclear distance. In Fig. 5(b), taking the 20th

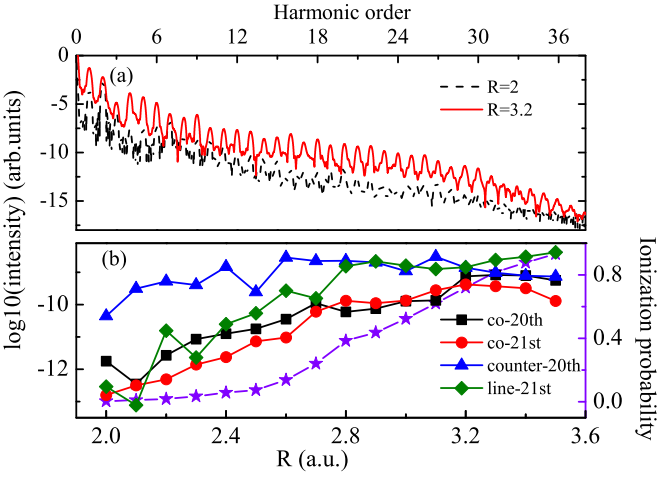

FIG. 5. (a) The harmonic spectrum comparison of H_2^+ at $R = 2$ (black line) and $R = 3.2$ (red line) in the co-rotating two-color circular polarization field. (b) The intensity comparison of the 20th-order (black square) and 21st-order (red circle) harmonics of H_2^+ in the co-rotating two-color circular polarization field at different internuclear distance, and the ionization probability as a function of the internuclear distance (five-pointed purple star). H_2^+ in the counter-rotating two-color circular polarization field of the 20th-order (blue triangle) and monochromatic linear polarization field of the 21st-order (red circle) harmonic intensity as a function of the internuclear distance.

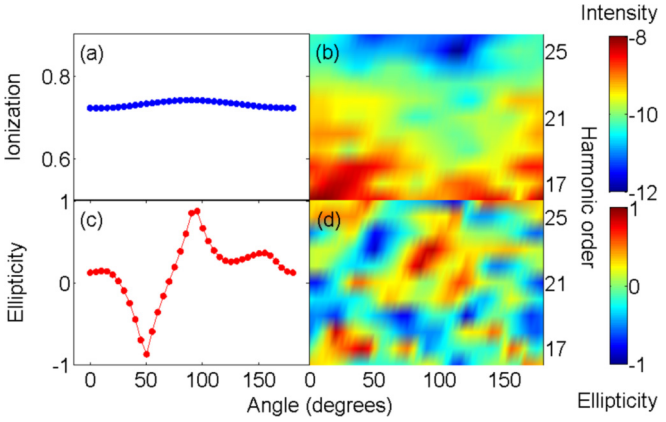

FIG. 6. (a) Ionization yield, (b) harmonic intensity in the plateau region, (c) 23rd harmonic ellipticity, and (d) harmonic ellipticity in the plateau as a function of the angle.

and 21st harmonics as examples, we examined the harmonic intensity as a function of the internuclear distance. After increasing the internuclear distance, the harmonic intensity is gradually increased, and the harmonic intensity is strongest when the internuclear distance is $R = 3.2$. However, after further increasing the internuclear distance, the harmonic intensity is no longer increased and even begins to decline. The reason for the intensity changes with the internuclear distance can be understood by the molecular ionization. In Fig. 5(b) we gave the ionization probability of the molecule as a function of the internuclear distance by the CRTCCP field, as indicated by the five-pointed purple star. When the molecular internuclear distance is small and as the internuclear distance is increased, the ionization probability and intensity of the harmonic emission become higher. At the same time, the spatial scale of the molecule is gradually increased, and the recolliding probability for the ionized electron with the molecular nucleus is also enhanced; therefore, the harmonic intensity is increased. However, with a large enough internuclear distance, the ionization potential of the electrons in the molecule will decrease less. Under the action of the laser field, ionization saturation occurs in the molecule. The electrons of the molecule are rapidly ionized and become vacant near the nucleus in the rising edge of the pulse field. Since the generation of higher harmonics is a process of excited recombination [39], the depletion of the ground-state electrons will lead to a decrease in harmonic intensity. In addition, we conducted a harmonic intensity comparison of the H_2^+ generated by the co-rotating two-color and counter-rotating two-color circularly polarized fields and monochromatic linearly polarized field, as shown in Fig. 5(b). At $R = 3.2$, the harmonic intensity under the co-rotating two-color circularly polarized field is comparable to that of the counter-rotating two-color circularly polarized field (blue triangle) and the monochromatic linearly polarized field (green diamond), and in another calculation range under the internuclear distance, the harmonic intensity under the co-rotating two-color circularly polarized field is weak.

The harmonic intensity is affected not only by the molecular internuclear distance but also by the angle θ between the molecular axis and the laser electric field vector. Figure 6 shows the ionization yield of H_2^+ [Fig. 6(a)], the harmonic

intensity in the plateau region [Fig. 6(b)], the 23rd harmonic ellipticity [Fig. 6(c)], and the harmonic ellipticity in the plateau as a function of angle θ [Fig. 6(d)]. As shown in Fig. 6(a), the ionization yield has little change with the varying of the alignment angle, and the variation of the harmonic intensity with the alignment angle is attributed to the recollision probability of the ionized electron. As the angle θ increases, the harmonic intensity can be changed, and the intensities of the high-order harmonics are weaker near $\theta = 120^{\circ}$, which can be observed in Fig. 6(b). The effect of the alignment angle on the harmonic intensity is weaker than that of the amplitude ratio and the molecular internuclear distance on the harmonic intensity. The harmonic ellipticity of the plateau region at different angles is shown in Figs. 6(c) and 6(d). In this figure, the ellipticity is represented by color. The right circular polarization is $+1$, and the left circular polarization is -1. The harmonic ellipticity can be calculated by $e = (|a_+| - |a_-|)/(|a_+| + |a_-|)$, where $a_\pm = \frac{1}{\sqrt{2}}(a_x \pm i a_y)$. a_x and a_y are the x and y components of the dipole acceleration in the frequency domain, respectively [26,40]. The harmonic ellipticity is significantly affected by the molecular alignment angle. As the molecular alignment angle is changed, the high-order harmonics are converted among the left circular, linear, and right circular polarizations.

IV. CONCLUSIONS

In summary, we numerically studied the harmonic generation of H_2^+ in the CRTCCP laser pulse. The simulated results showed that the amplitude ratio of the CRTCCP laser pulse has an impact on harmonic intensity. When the amplitude ratio is approximately 1:2.3, the harmonic intensity is generally higher. Furthermore, the harmonic intensity of H_2^+ is much higher than that of the atomic situation. By analyzing classical trajectory and the evolution of the electronic time-dependent wave packet, we found that the laser electric field amplitude ratio, the molecular internuclear distance, and the alignment angle directly affect the probability of the ionized electron recolliding with the parent ion, which correspondingly changes the harmonic emission intensity. Moreover, by adjusting the molecular alignment angle, the ellipticity of the harmonics of the plateau region can be controlled, and some harmonics can be converted among left circular, linear, and right circular polarizations. Therefore, this scheme can be used to generate a more intense and polarization controllable coherent high-frequency light source in experiments.

ACKNOWLEDGMENTS

This work was partially supported by the National Key Research and Development Program of China (Grants No. 2019YFA0307700 and No. 2017YFA0403300), the National Natural Science Foundation of China (NSFC) (Grants No. 11534004, No. 11627807, No. 11774175, No. 11774129, No. 11975012, and No. 11604119), the Jilin Provincial Research Foundation for Basic Research, China (Grant No. 20170101153JC), and the Science and Technology project of the Jilin Provincial Education Department (Grant No. JJKH20190183KJ). We acknowledge the High Performance Computing Center of Jilin University for supercomputer time.

[1] F. Krausz and M. Ivanov, Rev. Mod. Phys. **81**, 163 (2009).
[2] A. Pou and C. Serrat, EPJ Web Conf. **41**, 01001 (2013).
[3] T. Popmintchev *et al.*, Science **336**, 1287 (2012).
[4] T. Popmintchev, M.-C. Chen, P. Arpin, M. M. Murnane, and H. C. Kapteyn, Nat. Photon. **4**, 822 (2010).
[5] J. G. Chen, Y. J. Yang, S. L. Zeng, and H. Q. Liang, Phys. Rev. A **83**, 023401 (2011).
[6] J. G. Chen, S. L. Zeng, and Y. J. Yang, Phys. Rev. A **82**, 043401 (2010).
[7] P.-M. Paul, E. S. Toma, P. Breger, G. Mullot, F. Auge, P. Balcou, H. G. Muller, and P. Agostini, Science **292**, 1689 (2001).
[8] T. Gaumnitz, A. Jain, Y. Pertot, M. Huppert, I. Jordan, F. Ardana-Lamas, and H. J. Wörner, Opt. Express **25**, 27506 (2017).
[9] C. Jia, J. Wang, Q.-Y. Li, F.-M. Guo, J.-G. Chen, S.-L. Zeng, and Y.-J. Yang, Opt. Express **23**, 32222 (2015).
[10] J. Wang, G. Chen, S.-Y. Li, D.-J. Ding, J.-G. Chen, F.-M. Guo, and Y.-J. Yang, Phys. Rev. A **92**, 033848 (2015).
[11] Y.-T. Zhao, S.-Y. Ma, S.-C. Jiang, Y.-J. Yang, X. Zhao, and J.-G. Chen, Opt. Express **27**, 34392 (2019).
[12] E. V. van der Zwan and M. Lein, AIP Conf. Proc. **963**, 570 (2007).
[13] J. B. Bertrand, H. J. Wörner, P. Hockett, D. M. Villeneuve, and P. B. Corkum, Phys. Rev. Lett. **109**, 143001 (2012).
[14] M. C. H. Wong, A. T. Le, A. F. Alharbi, A. E. Boguslavskiy, R. R. Lucchese, J. P. Brichta, C. D. Lin, and V. R. Bhardwaj, Phys. Rev. Lett. **110**, 033006 (2013).
[15] J. Chen, Y. Yang, J. Chen, and B. Wang, Phys. Rev. A **91**, 043403 (2015).
[16] P. B. Corkum, Phys. Rev. Lett. **71**, 1994 (1993).
[17] M. Lewenstein, P. Balcou, M. Y. Ivanov, A. L'Huillier, and P. B. Corkum, Phys. Rev. A **49**, 2117 (1994).
[18] M. Möller, Y. Cheng, S. D. Khan, B. Zhao, K. Zhao, M. Chini, G. G. Paulus, and Z. Chang, Phys. Rev. A **86**, 011401(R) (2012).
[19] K. S. Budil, P. Salières, A. L'Huillier, T. Ditmire, and M. D. Perry, Phys. Rev. A **48**, R3437(R) (1993).
[20] H. Eichmann, A. Egbert, S. Nolte, C. Momma, B. Wellegehausen, W. Becker, S. Long, and J. K. McIver, Phys. Rev. A **51**, R3414(R) (1995).
[21] O. Kfir *et al.*, Nat. Photon. **9**, 99 (2014).
[22] D. D. Hickstein *et al.*, Nat. Photon. **9**, 743 (2015).
[23] L. Medišauskas, J. Wragg, H. van der Hart, and M. Y. Ivanov, Phys. Rev. Lett. **115**, 153001 (2015).
[24] S. Odžak, E. Hasović, and D. B. Milošević, Phys. Rev. A **94**, 033419 (2016).
[25] Á. Jiménez-Galán, N. Zhavoronkov, M. Schloz, F. Morales, and M. Ivanov, Opt. Express **25**, 22880 (2017).
[26] X. Zhang, X. Zhu, X. Liu, D. Wang, Q. Zhang, P. Lan, and P. Lu, Opt. Lett. **42**, 1027 (2017).
[27] S. Long, W. Becker, and J. K. McIver, Phys. Rev. A **52**, 2262 (1995).
[28] D. B. Milošević, W. Becker, and R. Kopold, Phys. Rev. A **61**, 063403 (2000).

[29] P. Sharma, E. Agrawal, and P. Jha, Phys. Plasmas **25**, 093102 (2018).
[30] C. Huang, M. Zhong, and Z. Wu, Opt. Express **27**, 7616 (2019).
[31] M. Busuladžić, A. Čerkić, A. Gazibegović-Busuladžić, E. Hasović, and D. B. Milošević, Phys. Rev. A **98**, 013413 (2018).
[32] T. E. Sharp, At. Data Nucl. Data Tables **2**, 119 (1970).
[33] M. R. Hermann and J. A. Fleck, Jr., Phys. Rev. A **38**, 6000 (1988).
[34] T.-F. Jiang and Shih-I Chu, Phys. Rev. A **46**, 7322 (1992).
[35] J. Wang, G. Chen, F. M. Guo, S. Y. Li, J. G. Chen, and Y. J. Yang, Chin. Phys. B **22**, 033203 (2013).
[36] Y. J. Yang, J. G. Chen, Y. X. Huang, F. M. Guo, H. X. Zhang, J. Z. Sun, H. Y. Zhu, L. Wang, H. Wang, and Q. R. Zhu, Chin. Phys. Lett. **24**, 1894 (2007).
[37] F. M. Guo, Y. J. Yang, M. X. Jin, D. J. Ding, and Q. R. Zhu, Chin. Phys. Lett. **26**, 053201 (2009).
[38] R. Panfili, J. H. Eberly, and S. L. Haan, Opt. Express **8**, 431 (2001).
[39] A. Pukhov, S. Gordienko, and T. Baeva, Phys. Rev. Lett. **91**, 173002 (2003).
[40] S. Odžak and D. B. Milošević, Phys. Rev. A **92**, 053416 (2015).